Swiss J Geosci (2014) 107:49–64
DOI 10.1007/s00015-013-0156-2

Precambrian to Paleozoic zircon record in the Siviez-Mischabel basement (western Swiss Alps)

T. Scheiber · J. Berndt · K. Mezger · O. A. Pfiffner

Received: 22 February 2013 / Accepted: 2 December 2013 / Published online: 1 March 2014

Abstract U–Pb zircon analyses from three meta-igneous and two metasedimentary rocks from the Siviez-Mischabel nappe in the western Swiss Alps are presented, and are used to derive an evolutionary history spanning from Paleoarchean crustal growth to Permian magmatism. The oldest components are preserved in zircons from metasedimentary albitic schists. The oldest zircon core in these schists is 3.4 Ga old. Detrital zircons reveal episodes of crustal growth in the Neoarchean (2.7–2.5 Ga), Paleoproterozoic (2.2–1.9 Ma) and Neoproterozoic (800–550 Ma, Pan-African event). The maximum age of deposition for the metasedimentary rocks is given by the youngest detrital zircons within both metasedimentary samples dated at ~490 Ma (Cambrian-Ordovician boundary). This is in the age range of two granitoid samples dated at 505 ± 4 and 482 ± 7 Ma, and indicates sedimentation and magmatism in an extensional setting preceding an Ordovician orogeny. The third felsic meta-igneous rock gives a Permian age of intrusion, and is part of a long-lasting Variscan to post-Variscan magmatic activity. The zircons record only minor disturbance of the U–Pb system during the Alpine orogeny.

Keywords Geochronology · Siviez-Mischabel nappe · Randa orthogneiss · LA-ICP-MS · Zircon

Editorial handling: E. Gnos.

Electronic supplementary material The online version of this article (doi:10.1007/s00015-013-0156-2) contains supplementary material, which is available to authorized users.

T. Scheiber (✉)
Norwegian Geological Survey (NGU), Leiv Eirikssons vei 39, 7040 Trondheim, Norway
e-mail: thomas.scheiber@ngu.no

J. Berndt
Institut für Mineralogie, Westfälische-Wilhelms Universität Münster, Corrensstraße 24, 48149 Münster, Germany

K. Mezger · O. A. Pfiffner
Institute of Geological Sciences, University of Bern, Baltzerstrasse 1+3, 3012 Bern, Switzerland

1 Introduction

The pre-Triassic crystalline basement units assembled in the Alpine collision zone are largely polycyclic. Crustal material was multiply reworked and metamorphosed during several tectonic cycles involving orogenic processes with magmatic and metamorphic events. Pre-Alpine events recognized in the Alpine realm commonly belong to two Paleozoic orogenic cycles. (1) A Cambrian to Ordovician cycle (500–440 Ma) is represented by a number of felsic and mafic intrusions in many pre-Alpine basement units (e.g., Neubauer 2002: von Raumer et al. 2002, 2013; Bussien et al. 2011; Cavargna-Sani et al. 2013). Furthermore, eclogites defining a high pressure subduction stage have been recognized in a few pre-Alpine basement units and have been attributed to this same orogenic cycle (Pfeifer et al. 1993; Rubatto et al. 2001; Schaltegger et al. 2003). The timing of this orogenic cycle is coeval with the Caledonian orogeny in northwestern Europe (e.g., Krawczyk et al. 2008), but the relationship between the Cambrian to Ordovician events recognized in Alpine basement units and the Caledonian orogen sensu stricto is not entirely clear. (2) The Variscan cycle (Carboniferous-Permian, 350–270 Ma) has been recognized in most pre-Alpine basement units and has mainly reached conditions of the amphibolite facies (Schaltegger 1997; von Raumer et al. 2009). Evidence for Variscan eclogite metamorphism is scarce in Europe (Franke 2006; Kroner et al. 2008).

However, in the Alpine realm a Variscan age for eclogitization has been proposed for Penninic basement units of the Ligurian Alps (Giacomini et al. 2007) and for Austroalpine basement domains of the Eastern Alps (Thöni 2006, and references therein). Volumetrically large magmatic bodies, related to the Variscan orogeny and post-orogenic collapse, were emplaced all over Central Europe, including the pre-Alpine basement units (e.g., Bonin et al. 1993; Finger et al. 1997). In addition to these two major orogenic cycles that are recorded in mineral parageneses and deformation features there is evidence from inherited zircon grains for even older material that was substantially reworked during the Paleozoic (e.g., Gebauer et al. 1989; Schulz 2008).

The U–Pb laser ablation inductively coupled plasma mass spectrometry (LA-ICP-MS) analysis of zircon is a powerful tool to decipher the chronology of polyphase orogenic cycles. In-situ analysis allows targeting small volumes of specific zones in a zircon crystal and thus provides high spatial resolution of down to a few micrometer (e.g., Bowring et al. 2006; Kooijman et al. 2012). In this study we present U–Pb LA-ICP-MS zircon data from meta-igneous and metasedimentary rocks from the pre-Alpine basement units of the Siviez-Mischabel nappe (Penninic domain of western Switzerland, Fig. 1), which provide evidence for both the Cambrian-Ordovician and the Carboniferous-Permian magmatometamorphic cycles. We show that not all meta-igneous basement slices in the

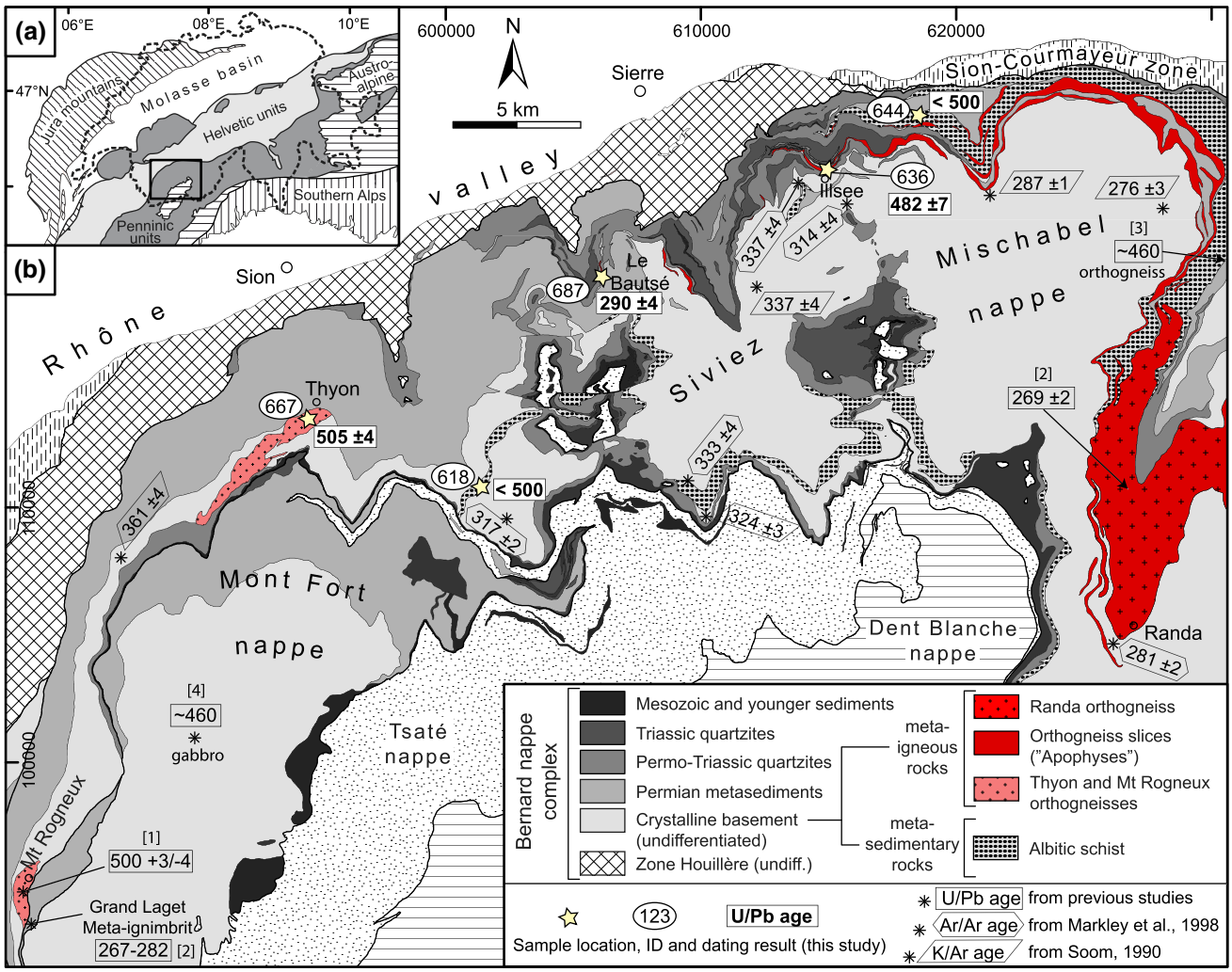

Fig. 1 **a** Location of the study area. **b** Geological map of the study area compiled on the basis of maps by Bearth (1978), Thélin (1987), Sartori and Thélin (1987), Escher (1988), Steck et al. (1999), Sartori et al. (2006), Genier et al. (2008), Gabus et al. (2008a), Marthaler et al. (2008), Sartori et al. (2011) and own observations. Legend covers units of the Bernard nappe complex only. Zircon U–Pb dating results from this study, from [1] Bussy et al. (1996a), [2] Bussy et al. (1996b), [3] Genier et al. (2008) and [4] Gauthiez et al. (2011) are presented in rectangles. For meta-igneous rocks intrusion ages (in Ma) are given, whereas maximum deposition ages (in Ma) are given for metasediments. Ar/Ar and K/Ar ages (in Ma) from white micas forming the main foliation in the crystalline basement (Soom 1990; Markley et al. 1998) are also given

frontal part of the Siviez-Mischabel nappe are related to the Permian Randa orthogneiss as suggested earlier (e.g., Marthaler et al. 2008). In addition, the data show that rocks, previously interpreted as meta-igneous, probably have a sedimentary origin, and their detrital zircon age spectra help constrain their maximum depositional ages. Furthermore we present the first age of the main body of the Thyon orthogneiss and discuss the data in relation to the timing of pre-Cambrian magmatic cycles, the Cambrian to Ordovician orogenic cycle and the Carboniferous to Permian (Variscan) evolution in basement units of the Alpine realm.

2 Geological setting

The Siviez-Mischabel nappe makes up the biggest part of the Bernard nappe complex, which constitutes the middle Penninic nappe system exposed in western Switzerland (Fig. 1). Paleogeographically, this nappe complex derives from the Briançon domain (e.g., Ellenberger 1952; Sartori 1987b, 1990; Stampfli et al. 1998). It consists of a complex assemblage of crustal slices which under- and overlies Permo-Mesozoic metasediments (Fig. 1b). Alpine metamorphism reached greenschist to blueschist facies conditions (Bousquet et al. 2004; Oberhänsli et al. 2004). The rocks of the Siviez-Mischabel nappe can be grouped into polymetamorphic and monometamorphic lithologies.

The pre-Permian polymetamorphic basement contains a variety of paragneisses and micaschists, interlaced with amphibolite and minor eclogite bodies (Sartori and Thélin 1987; Thélin 1989; Thélin et al. 1990, 1993; Rahn 1991; Sartori et al. 2006), as well as meta-igneous rocks including metagranites (Zingg 1989; Bussy et al. 1996a) and metagabbros (Sartori 1990). The polymetamorphic meta-igneous rocks occur as two larger bodies (Thyon and Mt Rogneux orthogneiss; Fig. 1b), as well as many discontinuous, thin bodies (less than 20 m thick), that are widely distributed within the polymetamorphic basement, but are not shown in Fig. 1b due to their small size. Relics of pre-Alpine metamorphic assemblages have been described from all parts of the Siviez-Mischabel nappe. However, the timing of these metamorphic events is not entirely resolved so far (e.g., Thélin et al. 1993; Sartori and Epard 2011).

The monometamorphic lithologies record Alpine metamorphism only and can be subdivided into two groups: granites associated with the post-Variscan Randa orthogneiss (Fig. 1b; 269 ± 2 Ma U–Pb on zircon; Bearth 1963; Thélin 1987; Bussy et al. 1996b; Genier et al. 2008) and Permian-Mesozoic metasediments. The Permian-Mesozoic metasedimentary sequence starts with mainly quartz-rich conglomerates, schists, metamorphosed volcaniclastic rocks and metapelites of Permian age (Vallet 1950; Schaer 1959; Burri 1983). Permo-Triassic quartzites lie either stratigraphically on top of the Permian sediments or directly on crystalline basement units. In the eastern part of the study area, fragments of the Mesozoic and younger, carbonate-dominated sequences are still preserved on top of the quartzites (Fig. 1b, Barrhorn and Toûno series after Ellenberger 1953; Sartori 1987a). The timing of Alpine nappe stacking is constrained by $^{40}Ar/^{39}Ar$ ages of synkinematically grown micas dated at 41–36 Ma (Markley et al. 1998, 2002).

3 Description of the investigated samples

Different rock types were sampled, three of which represent the variety of felsic meta-igneous rocks hosted by the Siviez-Mischabel nappe, and two are from the metasedimentary polymetamorphic basement (Fig. 1b).

3.1 Orthogneiss slices: samples 636 and 687

In the frontal part of the Siviez-Mischabel nappe, relatively thin orthogneiss slices occur within Permo-Mesozoic cover sequences (Fig. 1b). According to Markley et al. (1999) and own observations this is mainly the result of tectonic imbrication of basement slices and metasedimentary rocks during Alpine deformation. In the maps of the Geological Atlas of Switzerland (sheets Sierre, Gabus et al. 2008a; Vissoie, Marthaler et al. 2008) these orthogneisses are described as apophyses of the Randa orthogneiss, indicating that they could represent sheared-off smaller magmatic bodies or dikes related to this larger orthogneiss. The main body of the Randa orthogneiss is located in the eastern part of the Siviez-Mischabel nappe (Fig. 1b) and forms a pseudo-laccolith with sill-like apophyses. This orthogneiss represents a deformed subalkaline porphyritic granite (Thélin 1987) and was dated at 269 ± 2 Ma (U–Pb on zircon; Bussy et al. 1996b).

Sample 636 (north of Illsee) comes from an approximately 50 m thick orthogneiss slice, which is sandwiched between Permo-Triassic quartzites (Fig. 1b). It is located relatively close to the main body of the Randa orthogneiss and associated branches. However, this proximity by itself is not an argument for the age of the rock. The orthogneiss contains K-feldspar clasts (up to 3 cm in diameter, some broken), which are aligned in a commonly well-developed foliation together with quartz, white mica and chlorite. This foliation is subparallel to the lithological contacts, but in areas where it is weak, an older fabric can locally be observed.

Sample 687 (north of Le Bautsé) was taken from a ~15 m thick orthogneiss slice that is over- and underlain by Permo-Triassic quartzites. This rock is macro- and microscopically similar to sample 636, except that no older fabric was observed.

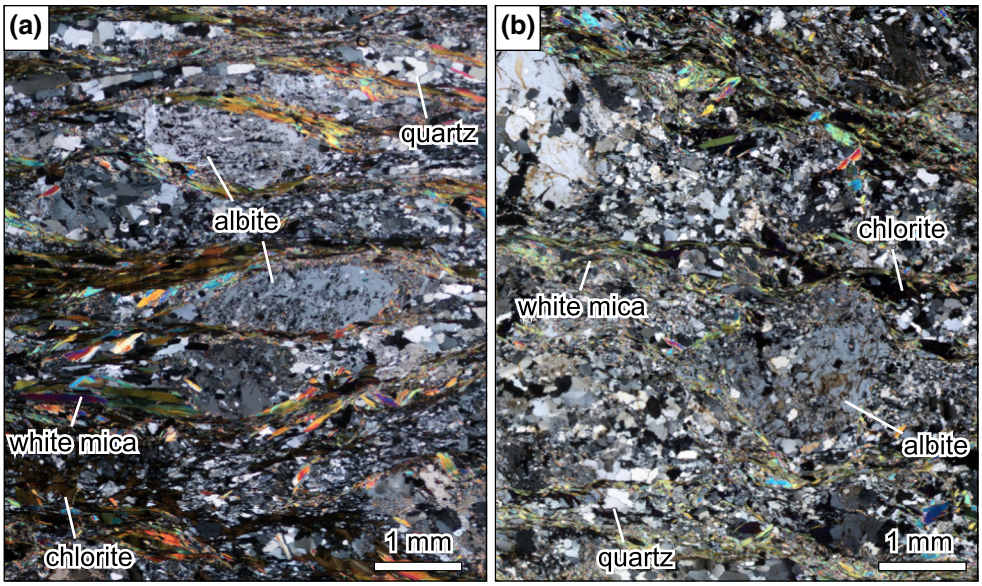

Fig. 2 Photomicrographs of representative mineralogy observed in the two metasedimentary samples 618 (**a**) and 644 (**b**). Albite porphyroblasts show an internal foliation defined by epidote, quartz and sericite

3.2 Thyon orthogneiss: sample 667

The Thyon orthogneiss crops out in the western part of the study area (Fig. 1b). According to Burri et al. (1992) the Thyon orthogneiss belongs to the same magmatic suite as the Mont Rogneux orthogneiss (Fig. 1b), which was dated at 500 +3/−4 Ma (U–Pb on zircon; Bussy et al. 1996a). Sample 667 was taken from a biotite-metagranite at the Thyon locality. It shows a weak steeply N-dipping main foliation, which is overprinted by shear bands close to the base of the nappe, indicating top-to-the-north Alpine movement (Scheiber et al. 2013b).

3.3 Albitic schist: samples 618 and 644

Within the Siviez-Mischabel basement, there are several zones of albite-rich schists (Fig. 1b). Sample 618 (Fig. 1b) comes from a zone called SOPA ("**S**chistes **O**eillés à **P**orphyroblastes d'**A**lbite", Sartori and Thélin 1987), whereas the zone around sample 644 (Fig. 1b) has been named Bielen unit (Thélin 1987; Genier et al. 2008). However, our field observations indicate that the two zones consist of very similar rocks. They are characterized by albite porphyroblasts occurring within a granolepidoblastic matrix of predominantly quartz, white mica and chlorite (Fig. 2). The albite porphyroblasts bear an internal foliation mainly defined by small crystals of epidote, quartz and sericite that are variably oriented with respect to the main foliation in this rock (Fig. 2a, see also Sartori and Thélin 1987).

The SOPA zone (sample 618) overlies banded amphibolites with eclogite facies relics, and hosts itself boudins of amphibolite and eclogite (Thélin et al. 1990; Sartori et al. 2006). In addition, thin porphyritic and leucocratic orthogneiss layers (max. 15 m thick) can be commonly observed at the border between SOPA and underlying amphibolites, as well as rarely within the SOPA (not shown in Fig. 1b due to their small size). The SOPA have been interpreted as semi-pelitic metasediments (Sartori and Thélin 1987). The main foliation in the SOPA is subparallel to that in the adjacent lithologies and to lithological contacts. It is vertically to steeply south-dipping in the internal part of the basement and turns into a moderately to slightly south-dipping orientation approaching the overlying parautochthonous cover. No radio-isotope ages have been published on this rock type, but a Proterozoic age of deposition was proposed on the basis of lithostratigraphic relationships (Sartori et al. 2006).

The sampled part of the Bielen unit (sample 644) represents an up to 400 m thick basement slice, which overlies Permian metasediments and is overlain by imbricated Permo-Triassic sediments. It occurs together with numerous orthogneiss bands (apophyses of the Randa orthogneiss according to Gabus et al. 2008b). The albite and quartz porphyroblasts are generally smaller than in the SOPA unit (<1 cm diameter) and occur in a matrix mainly composed of quartz, white mica and chlorite. Gabus et al. (2008b) speculated that this unit could represent a metarhyolite, associated with the emplacement of the Randa orthogneiss and, furthermore, could be an equivalent of the Rofna Porphyry Complex of eastern Switzerland. However, geochronological data testing this hypothesis is lacking so far.

4 Analytical methods

Conventional magnetic and heavy liquid techniques were used to separate zircons, which were in a further step handpicked under a binocular microscope. Individual crystals

were mounted in one-inch epoxy discs and polished down to expose the grain centers. Samples were characterized by backscatter electron (BSE) and cathodoluminescence (CL) imaging prior to analysis. The LA-ICP-MS analyses were performed using a ThermoScientific Element2 sector field ICP-MS coupled to a New Wave UP193HE ArF Excimer laser system at the Institut für Mineralogie, Universität Münster. An in-house produced low-volume ablation cell (following Bleiner and Günther 2001) was used to reduce washout time and increase signal intensities.

Masses ^{202}Hg, ^{204}Hg + ^{204}Pb, ^{206}Pb, ^{207}Pb and ^{238}U were acquired in e-scan mode. ^{207}Pb/^{235}U was calculated from ^{207}Pb/^{206}Pb and ^{206}Pb/^{238}U using the natural abundance for ^{238}U/^{235}U (the "consensus value" of 137.88; Steiger and Jäger 1977). A laser spot size of 35 µm and, in some cases, 25 µm and also 12 µm was used at energies of 5 J/cm^2 and a repetition rate of 10 Hz. The total ablation time per analysis was 52 s, including 12 s during which the shutter remained closed to measure the background (i.e. gas blank). Pre-ablation of all spots was performed to remove surface common Pb. Laser-induced elemental fractionation and instrumental mass bias were corrected by bracketing groups of 10 unknowns with 3 analyses of GJ1 zircon as standard reference material (Jackson et al. 2004). Along with the unknowns, the 91500 zircon (Wiedenbeck et al. 1995, 2004) was measured to monitor precision and accuracy of the analyses.

Data were processed following the procedure of Kooijman et al. (2012). A correction for common Pb (Stacey and Kramers 1975) was applied if the common ^{206}Pb of the total measured ^{206}Pb exceeded 1 %. All errors are reported at the 2σ-level and all uncertainties of weighted mean calculations are given as the 95 % confidence limit. The construction of concordia diagrams was performed using the Isoplot 3.71 program (Ludwig 2008). Single spot analyses are given as ^{207}Pb/^{206}Pb ages for results older than 1 Ga and ^{206}Pb/^{238}U ages for results younger than 1 Ga. The complete LA-ICP-MS data of all samples are given in a supplementary data table.

5 Zircon characteristics and U–Pb dating results

5.1 Sample 636: orthogneiss slice Illsee

Zircons separated from this sample are elongated to equant, mostly transparent, but some appear dirty due to a high density of cracks and inclusions. They are colorless to pink- or brownish, 120–320 µm long and 60–180 µm wide. Crystals are nearly euhedral but commonly exhibit slightly abraded edges. CL images reveal that this is due to the fact that all zircons are at least partly surrounded by an outermost CL-bright structureless rim that did not develop proper crystal faces (Fig. 3a). CL imaging furthermore reveals complex internal zircon textures with various core and rim generations. In some cases the zircon is broken and cracks are filled by the same bright material that makes up the outermost rim (D11 and G9, Fig. 3a). Eighteen out of twenty-nine analyzed spots are >90 % concordant (Fig. 4a). Analyses of two highly luminescent xenocrystic zircon cores give Neoproterozoic ^{206}Pb/^{238}U ages of 838 ± 31 and 714 ± 30 Ma, and another four analyses of sector-zoned moderately luminescent xenocrystic cores cluster between 622 ± 18 and 581 ± 16 Ma. The remaining 12 analyses with >90 % concordance cover a time span of about 30 Ma between 501 ± 12 and 470 ± 5 Ma and define a weighted mean ^{206}Pb/^{238}U age of 482 ± 7 Ma (MSWD = 4; Fig. 4a). No meaningful discordia line (two component mixing line) can be calculated for the analyses that are less than 90 % concordant (Fig. 4a). The CL-bright, very thin rims (Fig. 3a) were too thin to be analyzed with the 12 µm spot size of the laser beam.

5.2 Sample 687: orthogneiss slice Le Bautsé

Most zircons are elongate, prismatic and euhedral (Fig. 3b). They are clear, pink, and 140–360 µm long and 35–140 µm wide. Most zircons contain xenocrystic, variably zoned cores, overgrown by one or several mostly oscillatory zoned rims (Fig. 3b). They appear dirty in transmission microscopy, whereas zircons lacking a xenocrystic core are generally light pink and transparent. Many crystals are broken and fragmented. A total of 34 zircon spots were analyzed, but 26 analyses are less than 90 % concordant (Fig. 4b). One xenocrystic core is dated at 476 ± 10 Ma (D18, Fig. 3b), and four spot analyses spread from 291 ± 6 to 271 ± 7 Ma (^{206}Pb/^{238}U ages). Weighted mean calculations for a cluster of three analyses on three different crystals give 290 ± 4 Ma (MSWD 0.3) and 272 ± 4 Ma (MSWD 0.4) for two analyses (Fig. 4b). The two remaining concordant spots on two crystals yield ^{206}Pb/^{238}U ages of 249 ± 12 and 233 ± 7 Ma, respectively. Although no meaningful discordia lines can be calculated for the dataset less than 90 % concordant, a severe disturbance must have affected the U–Pb system after 290 Ma.

5.3 Sample 667: Thyon orthogneiss

Zircons from this rock are generally prismatic to equant and perfectly euhedral (Fig. 3c). They are colorless, clear, transparent, and 105–235 µm long and 60–115 µm wide. CL imaging reveals no xenocrystic cores, but a low

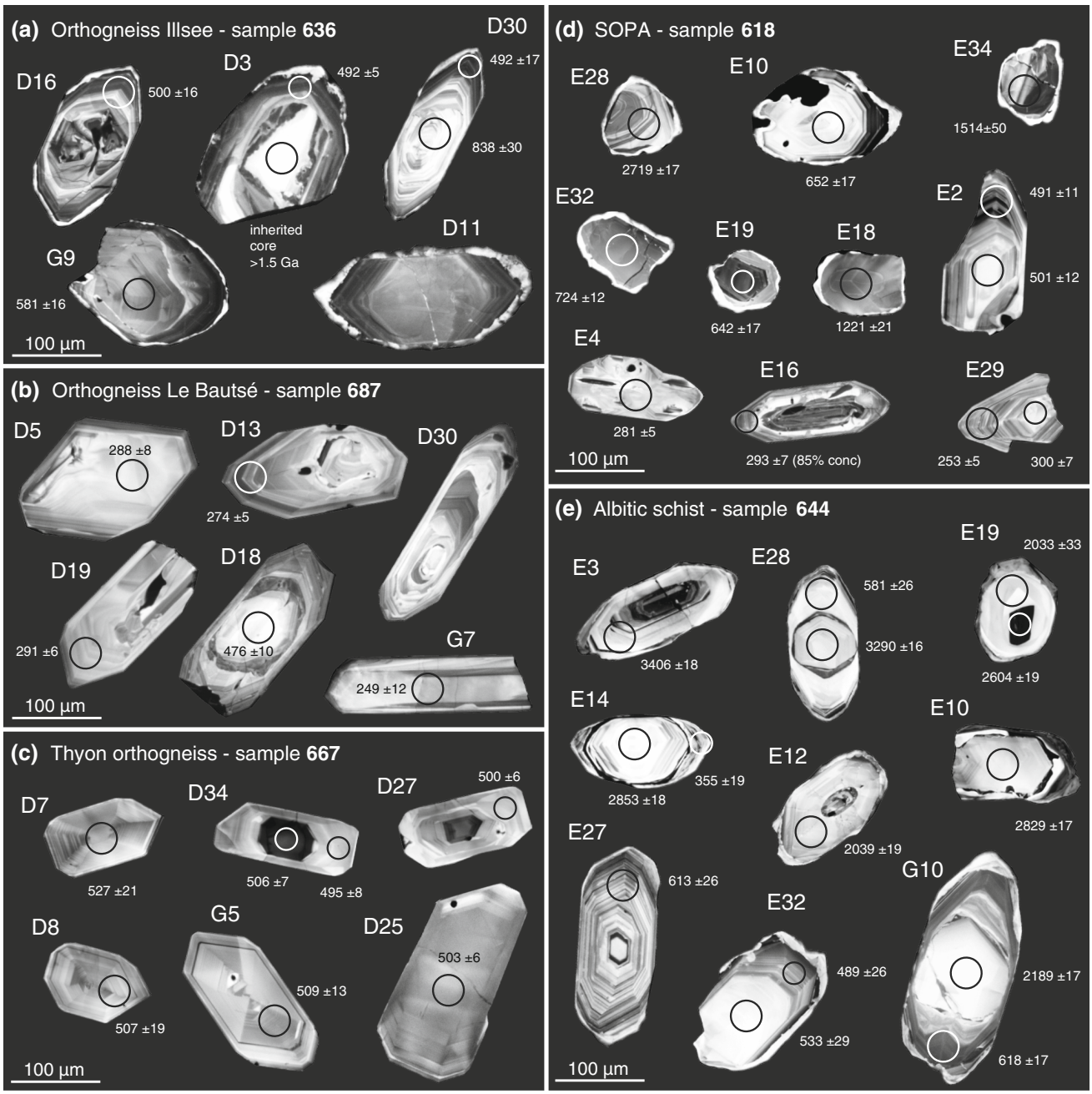

Fig. 3 Cathodoluminescence (CL) images of representative zircon crystals from three meta-igneous rocks (**a**–**c**) and two metasedimentary rocks (**d**, **e**) from the Siviez-Mischabel nappe. Scale is the same for all zircons. Analyzed spots are indicated by circles (diameter 35 and 25 µm). Obtained $^{206}Pb/^{238}U$ ages (Ma) are provided for results younger than 1 Ga, for analyses older than 1 Ga $^{207}Pb/^{206}Pb$ ages (Ma) are given. All errors are given at the 2σ-level

luminescent magmatic core and an isotropic brighter rim in some cases (Fig. 3c). There are no indications for resorption or overgrowth. Zircons display moderately to highly luminescent, planar zoned textures, which is typical of zircons precipitated during granite crystallization (e.g., Corfu et al. 2003). Only one out of 27 analyses is less than 90 % concordant. The 26 spot analyses (>90 % concordant) deriving from various parts within the zircons (core and rim areas) range between 537 ± 20 and 492 ± 20 Ma, and the calculated weighted mean $^{206}Pb/^{238}U$ age gives 505 ± 4 Ma (MSWD 2; Fig. 4c).

5.4 Sample 618: SOPA

Zircons have different colors (pinkish, brownish, colorless) and morphologies, i.e. they are broken, anhedral, rounded

or euhedral. Only few and relatively small zircons were extracted from this sample, with the biggest crystal being 200 µm long and 120 µm wide. CL imaging reveals that all but three zircons have an outermost highly luminescent rim, as similarly observed in the orthogneiss sample 636 (Fig. 3a, d). This rim is 0–25 µm wide and truncates cores, which are constituted by zircon fragments with various, complex internal core and rim textures, and thus already indicate different origins and multistage crystallization for the crystals. Similar highly luminescent zircon material can be observed in fissures cutting through the cores (E32 and E34, Fig. 3d). Nineteen of 24 analyses are more than 90 % concordant. Core areas gave ages ranging from (^{207}Pb/^{206}Pb) 2,719 ± 17 Ma to (^{206}Pb/^{238}U) 491 ± 11 Ma (Fig. 5a). Data cluster around 720, 640 and 500 Ma. Unfortunately analyses of the bright outermost rims did not deliver reasonable results because of unstable or too short signals. But for the three zircons lacking this outermost rim and showing a moderate to high luminescence, spot analyses yielded Carboniferous-Permian ^{206}Pb/^{238}U ages between 300 ± 7 and 253 ± 5 Ma (Fig. 5a). Zircon E16 is especially interesting because it shows a highly luminescent rim, which is irregularly overgrown by a moderately luminescent rim (Fig. 3d). One analysis of this rim gave a ^{206}Pb/^{238}U age of 293 ± 7 Ma (degree of concordance is 85 %). Again no meaningful discordia line could be calculated for the less than 90 % concordant analyses.

5.5 Sample 644: albitic schist

Zircons are up to 280 µm long and up to 140 µm wide. They have different shapes (broken, anhedral, rounded or euhedral) and colors (colorless, pale pink to brownish). CL images exhibit complex core- and rim-generations. Some crystals have an up to 20 µm wide outermost highly luminescent rim (e.g., E32, Fig. 3e), as also observed in samples 636 and 618. Forty-four analyses are more than 90 % concordant and 28 analyses are less than 90 % concordant. The color of zircons in transmitted light does not correlate with the age spectra. Nine analyses yielded Archean ages (Fig. 5b). One zircon spot was dated at 3,406 ± 18 Ma, one at 3,290 ± 16 Ma, a group of three analyses scatters around 2,835 Ma and another group of four analyses gave ages from 2,663 ± 30 Ma to 2,604 ± 19 Ma (^{207}Pb/^{206}Pb ages). Sixteen analyses point to Paleoproterozoic ^{207}Pb/^{206}Pb crystallization ages ranging from 2,363 ± 36 to 1,962 ± 26 Ma (Fig. 5b). The remaining 19 analyses yielded dates younger than 1 Ga (Fig. 5b), given as ^{206}Pb/^{238}U ages in the following. The majority of ages lie between 677 ± 18 and 581 ± 26 Ma. Three analyses yielded ages around 500 Ma. One analysis yielded an age of 355 ± 15 Ma for the outermost highly luminescent rim (Fig. 3e). There is a systematic arrangement of the less than 90 % concordant analyses in the concordia diagrams (Fig. 5b), pointing to lower intercepts of multiple discordia lines below 500 Ma. Furthermore three dates are younger than 300 Ma and discordant thus indicating a later disturbance of the U–Pb system.

6 Interpretation and discussion

U–Pb ages combined with zircon textures from both metaigneous and metasedimentary rocks from the Siviez-Mischabel nappe allow a reconstruction of the pre-Alpine magmatometamorphic evolution of this tectonic unit. Clearly, the composite nature of the zircon grains suggests a complex history of multiple crustal growth and accretion for parts of the Siviez-Mischabel basement. In the following, the various age groups recorded in the different samples (Figs. 4, 5, 6) are discussed and interpreted from the oldest to the youngest events.

6.1 Detrital zircon ages: Archean and Pan-African sources

Detrital zircon grains reflect the hinterland history of the sedimentary basins in which they were deposited and commonly show an episodic pattern, which can be interpreted in terms of continental crust formation cycles (e.g., Cawood et al. 2012). In order to make statistically sound statements about the presence or absence of certain age groups in a detrital age spectra, a certain amount of concordant analyses per sample is needed (i.e. >100 analyses per sample; e.g., Vermeesch 2004; Andersen 2005). Our data set contains 19 and 44 concordant analyses per metasedimentary sample, which is too little to be able to argue for the absence of any important population. Nevertheless, the presence of certain age populations in this data set can be discussed in a regional context. In addition, the youngest detrital grains within a sample can be used to estimate a maximum depositional age for this sample, which can be useful for sedimentary units lacking other stratigraphic age control (e.g., Dickinson and Gehrels 2009).

Figure 6 shows age probability plots for the age spectra of samples 618 and 644. Sample 618 is dominated by a detrital Paleozoic to Neoproterozoic population, with scattered Mesoproterozoic and one Archean analysis. Sample 644 contains a similar Paleozoic to Neoproterozoic population, but in addition contains large Paleoproterozoic and Archean populations. The two oldest analyses within this sample (^{207}Pb/^{206}Pb ages of 3.4 and 3.2 Ga, Paleoarchean) belong to the oldest zircons ever dated in the Central and Western Alps: similar ages are only reported from the Mont Fort nappe

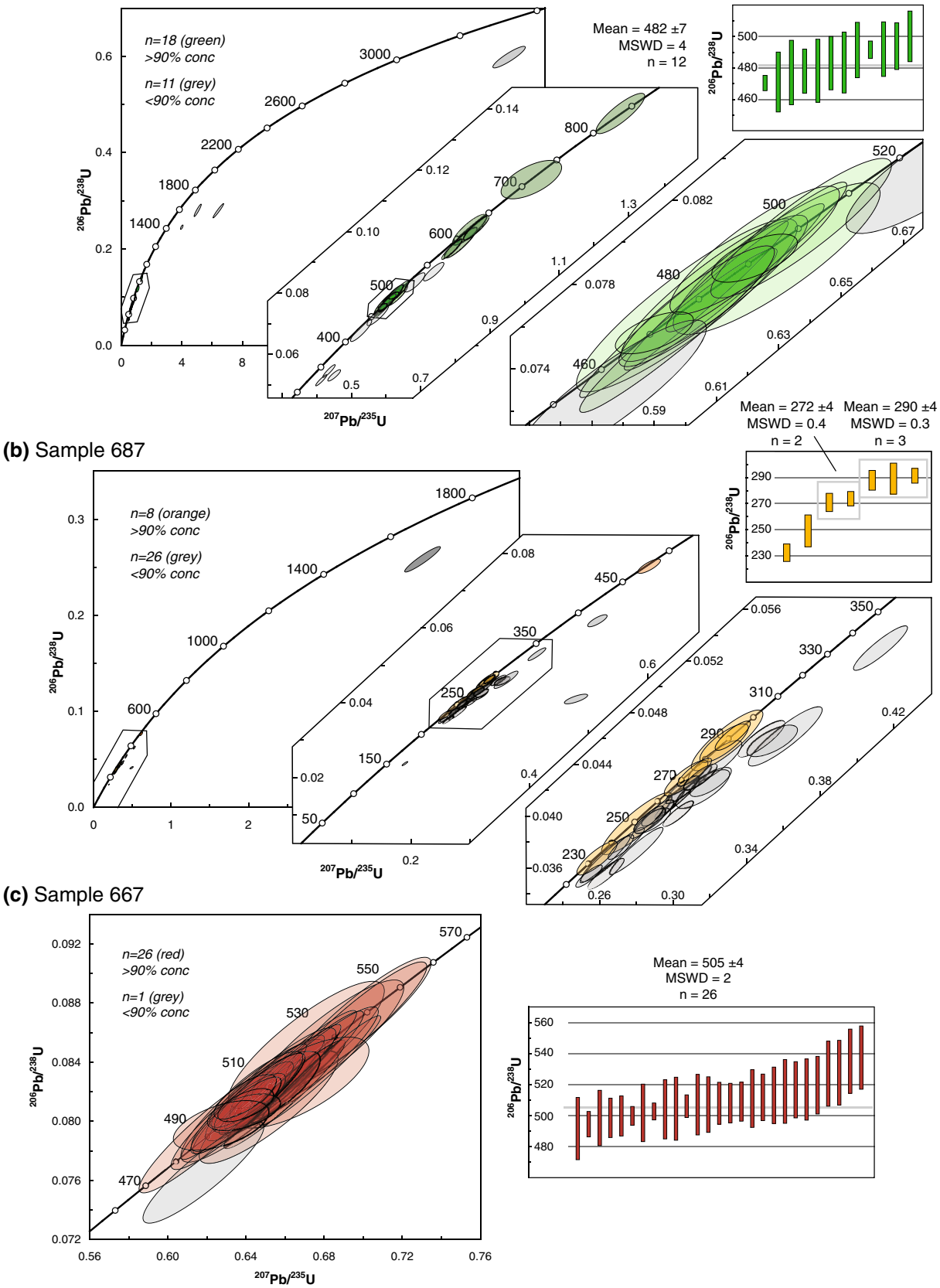
(a) Sample 636
n=18 (green)
>90% conc
n=11 (grey)
<90% conc
Mean = 482 ±7
MSWD = 4
n = 12
(b) Sample 687
n=8 (orange)
>90% conc
n=26 (grey)
<90% conc
Mean = 272 ±4
MSWD = 0.4
n = 2
Mean = 290 ±4
MSWD = 0.3
n = 3
(c) Sample 667
n=26 (red)
>90% conc
n=1 (grey)
<90% conc
Mean = 505 ±4
MSWD = 2
n = 26
206Pb/238U
207Pb/235U

◀**Fig. 4** Zircon U–Pb concordia plots for three igneous rock samples from the Siviez-Mischabel nappe. Weighted mean calculations are presented for populations of more than 90 % concordant analyses. **a** The orthogneiss slice of Illsee (636) shows a Cambrian-Ordovician crystallization age. **b** The orthogneiss slice from Le Bautsé (687) is related to the Permian magmatic activity of the Randa intrusion. **c** The Thyon orthogneiss (667) shows a Cambrian age of intrusion. Colored ellipses correspond to more than 90 % concordant data, gray ellipses to less than 90 %. Errors are reported at the 2σ-level

(3.5 Ga, Gauthiez et al. 2011) and from the Helvetic Gotthard massive (3.4 Ga, Gebauer 1993).

These Paleoarchean ages present in sample 644, together with the three Mesoarchean ages scattering around 2,850 Ma in the same sample are older than the oldest megacycle of crustal growth which is observed within the European Variscides from ~2.7 to 2.5 Ma (e.g., Gebauer et al. 1989). Our data indicate that at least some remnants of these old rocks found their way into the pre-Alpine basement units.

The next younger age population is represented by ages ranging from 2,663 ± 30 to 2,604 ± 19 Ma in sample 644 together with the oldest zircon from sample 618 (2,719 ± 17 Ma). These $^{207}Pb/^{206}Pb$ ages fit both the first megacycle of crustal growth observed within the European Variscides (e.g., Gebauer et al. 1989) and the oldest prominent age population of the N-Gondwana margin detritus (Meinhold et al. 2013). Furthermore these ages correspond to the major episode of continental crust formation in Earth's history (e.g., Taylor and McLennan 1985). The next younger $^{207}Pb/^{206}Pb$ age population in sample 644 (2,223 ± 17 to 1,962 ± 26 Ma) fits a second megacycle which occurred within the basement units of Central Europe during the Paleoproterozoic between ~2.2 and 1.9 Ga (Gebauer et al. 1989; Abouchami et al. 1990; Boher et al. 1992; Fernández-Suárez et al. 2002). The third prominent megacycle of the Central European basement units (1.2–0.9 Ga) is poorly represented in our data by three analyses (1,221 ± 21 and 1,027 ± 20 Ma, sample 618; 944 ± 27 Ma, sample 644).

The youngest detrital age populations (Neoproterozoic to Paleozoic) from both samples fit the well-known latest Precambrian megacycle associated with the assembly of Gondwana during the Pan-African (Cadomian) orogeny covering the time period from 800 to 550 Ma (Jackson and Ramsay 1980; Gebauer 1993; Rino et al. 2008; Timmerman 2008). Zircon cores from sample 618 even show evidence for two distinct crystallization pulses in the course of this Pan-African cycle at ~715 and ~640 Ma (Fig. 5a). Similar Neoproterozoic ages also occur as xenocrystic cores within the meta-igneous sample 636 (Fig. 4a) and thus reveal a strong influence of the Pan-African orogenic cycle on the development of the Siviez-Mischabel basement unit.

A provisional maximum age of deposition is provided by the youngest detrital zircon age. In sample 618 only the zircons showing a highly luminescent outermost rim are interpreted as detrital (Fig. 3d). The youngest analysis of such a zircon yields a Cambrian $^{206}Pb/^{238}U$ age of 491 ± 11 Ma (E2 in Fig. 3d). For sample 644 the youngest zircon interpreted as detrital was dated at ($^{206}Pb/^{238}U$) 489 ± 26 Ma (zircon E32 in Fig. 3e). This indicates that both metasediments possibly have latest Cambrian maximum depositional ages. This is younger than previously assumed by Sartori et al. (2006), who, based on lithostratigraphic arguments, placed the SOPA into the Proterozoic. However, the relationship of these sediments to the various Cambrian to Ordovician intrusions in this area is not entirely clear. Nevertheless, the detrital zircon age spectra of the two metasedimentary samples could reveal something about the tectonic setting, in which they were deposited. According to Cawood et al. (2012) the predominance of significantly older age spectra than the maximum depositional age points to an extensional setting during deposition. Extension is held responsible for the exhumation of older rocks in the source area.

6.2 The Cambrian-Ordovician evolution

The zircons from the Thyon metagranite (sample 667) show no inheritance and give a Cambrian $^{206}Pb/^{238}U$ magmatic crystallization age of 505 ± 4 Ma (Fig. 3c). This age is identical within error to the age of the Mt Rogneux orthogneiss (Fig. 1b), consistent with the hypothesis that these two magmatic bodies are derived from the same source, which was proposed by Burri et al. (1992) and Bussy et al. (1996a). The orthogneiss slice near Illsee (sample 636) yields an early Ordovician $^{206}Pb/^{238}U$ intrusion age of 482 ± 7 Ma (Fig. 4a) and thus was previously wrongly considered as "apophysis" of the Randa orthogneiss (e.g., Marthaler et al. 2008).

Cambrian-Ordovician ages of meta-igneous rocks are known from all over the European Variscan basement (e.g., Pin et al. 2007; Ballèvre et al. 2012; Díez Fernández et al. 2012). There are several occurrences within the pre-Alpine basement of the Alps (Neubauer 2002; von Raumer et al. 2013, and references therein), and ages around ~500 Ma (Cambrian) are relatively common in Briançon-derived basement units of the Central and Western Alps. In fact, such ages are reported from other localities within the Bernard nappe complex (Zingg 1989), also SE of the study area (Mont Rogneux orthogneiss, Bussy et al. 1996a; metagranophyre from Val de Rhèmes, Bertrand et al. 2000a), but also from the Suretta nappe of eastern Switzerland (Scheiber et al. 2013). Another set of Ordovician intrusion ages covering the time span between 480 and 440 Ma is known from the Bernard nappe complex

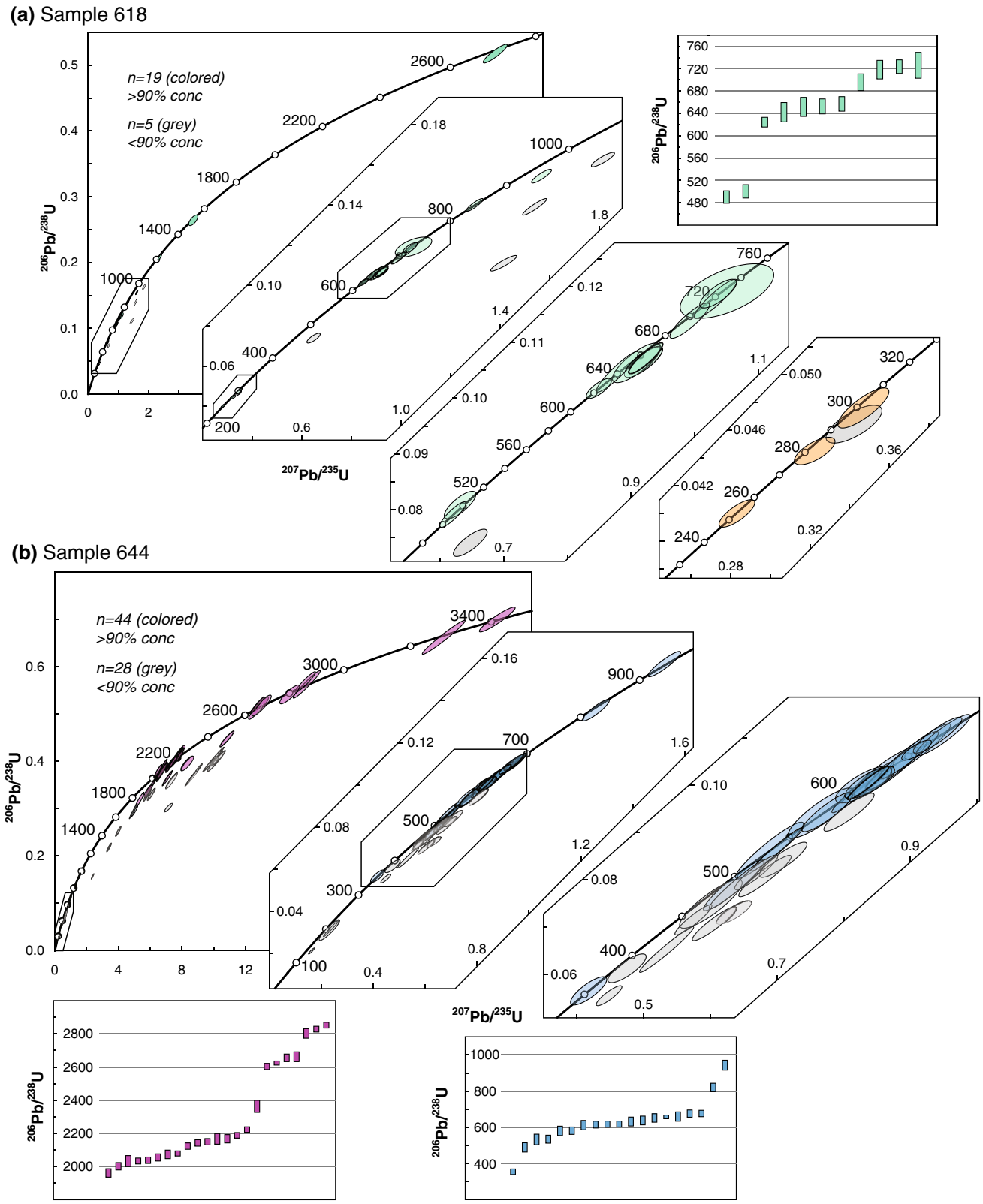
(a) Sample 618
n=19 (colored)
>90% conc
n=5 (grey)
<90% conc
206Pb/238U
207Pb/235U
(b) Sample 644
n=44 (colored)
>90% conc
n=28 (grey)
<90% conc
206Pb/238U
207Pb/235U

◀**Fig. 5** Zircon U–Pb concordia plots for two metasedimentary rock samples from the Siviez-Mischabel nappe. **a** Analyses of core areas from sample 618, shown in *green*, give Archean and Proterozoic ages. Three Carboniferous-Permian (*yellow*) data correspond to spots on zircons lacking a highly luminescent rim. **b** The age spectrum obtained from sample 644 can be grouped into ages >1 Ga (*violet*) and <1 Ga (*blue*). The two oldest and the one youngest dating results are not included in the "staircase" plots. Colored ellipses correspond to more than 90 % concordant data, gray ellipses to less than 90 %. Errors are reported at the 2σ-level

(Bertrand et al. 2000b; Guillot et al. 2002; Genier et al. 2008; Gauthiez et al. 2011), the Dora Maira massif (Bussy and Cadoppi 1996), and also from other Alpine basement units (e.g., Schaltegger and Gebauer 1999; Schaltegger et al. 2003; Bussien et al. 2011; Cavargna-Sani et al. 2013). Intrusions with an age interval between 520 and 480 Ma have been commonly interpreted to be the result of anorogenic magmatic activity associated with the continental break-up of Gondwana, particularly rifting processes along the north-Gondwana margin (e.g., von Raumer et al. 2002, 2003; Galli et al. 2012). The younger granitoid intrusions (480–440 Ma) were probably generated in a common orogenic setting (e.g., Guillot et al. 2002; Schaltegger et al. 2003).

No radio-isotope ages exist on the eclogite occurrences within the Siviez-Mischabel nappe and nothing about their evolution can be deduced from the data in the present study, except that the incorporation of high pressure relics in the metasedimentary rocks must have occurred later than ~490 Ma (which is the maximum depositional age for the surrounding sediments). However, the intrusion of gabbros within the Mont Fort nappe was dated at ~460 Ma (Fig. 1b; Gauthiez et al. 2011), indicating that their eclogitization must have occurred after that time. In the Helvetic basement (Aar and Gotthard massifs), similar eclogitized gabbros occur with intrusion ages of 467–478 Ma (Oberli et al. 1994; Schaltegger et al. 2003). There, the timing of the eclogite facies metamorphic overprint is bracketed by the intrusion age of the gabbros

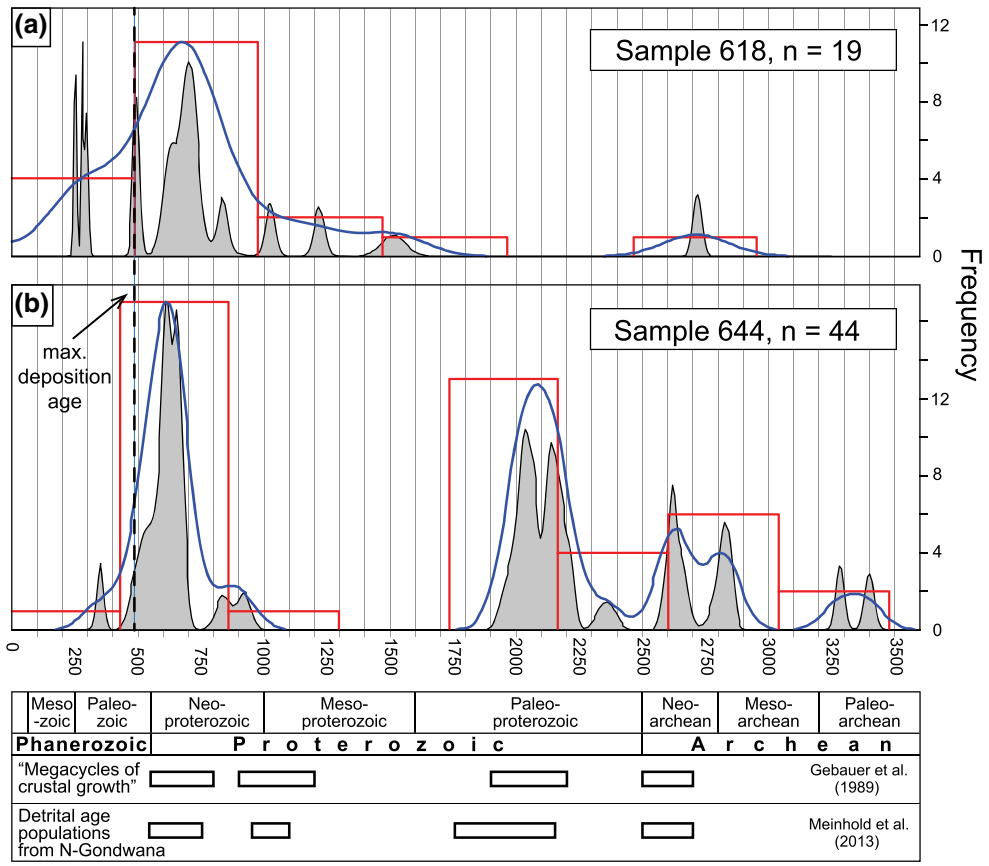

Fig. 6 Illustration of combined diagrams including probability density plots (*gray shaded*), frequency histograms (*red*) and kernel density estimations (*blue*) of $^{206}Pb/^{238}U$ ages (<1 Ga) and $^{207}Pb/^{206}Pb$ ages (>1 Ga), respectively, for the metasedimentary samples 618 (**a**) and 644 (**b**). Plots were created using the DensityPlotter of Vermeesch (2012). Diagrams indicate age distribution of concordance-filtered data at >90 %. The dashed line marks the maximum depositional age for both samples at ~490 Ma. Younger ages correspond to either bright rims or newly formed zircons, grown during Carboniferous to Permian magmatometamorphic events. In the lowest row, periods of increased crustal growth detected within the Central European basement units (Gebauer et al. 1989) and important detrital age populations from the northern Gondwana mainland (Meinhold et al. 2013) are depicted for comparison

and the emplacement of late Ordovician (~440 Ma) granitoids (e.g., Biino 1995), suggesting that the eclogites form part of an Ordovician orogenic cycle. This could also be the case for the eclogites of the Bernard nappe complex, which show a similar magmatic and metamorphic history with the bordering basement units (Pfeifer et al. 1993). Ordovician eclogitization in the Bernard nappe complex has already been proposed earlier by Thélin et al. (1990) and Eisele et al. (1997). However, Rubatto et al. (2010) presented evidence for Carboniferous (~338 Ma) high-pressure metamorphism of Ordovician protoliths in the Argentera Massif and Giacomini et al. (2007) documented Ordovician protolith and Devonian to Carboniferous (392–376 Ma) metamorphic zircon ages from one eclogite sample of the Ligurian Alps. Similarly there occur mafic to ultramafic rocks with probable Ordovician protoliths and Carboniferous metamorphic ages in the Tauern Window (von Quadt 1992). This opens up the possibility that some of the eclogites in the Bernard nappe complex could conceivably be Carboniferous (Variscan) eclogites as well.

6.3 Variscan and post-Variscan evolution

The main foliation commonly observed in basement rocks of the Siviez-Mischabel nappe today is represented by a greenschist-facies metamorphic paragenesis with local relict amphibolite facies assemblages (Bearth 1963; Thélin et al. 1993; Sartori et al. 2006). The age of this metamorphic overprint has been dated at 337 ± 4 to 276 ± 3 Ma (Fig. 1b, largest fraction white mica $^{40}Ar/^{39}Ar$ ages by Markley et al. 1998, and K/Ar ages by Soom 1990). The main foliation is thus of pre-Alpine age. One older age (361 ± 4 Ma) occurs in the west of the Siviez-Mischabel nappe (Fig. 1b). These data are in agreement with other published ages from the Briançon-derived basement of the Western Alps and are interpreted to reflect Variscan overprint (e.g., $^{40}Ar/^{39}Ar$ ages by Monié 1990; Giorgis et al. 1999). In addition, a U–Pb age of 330 ± 2 Ma was obtained from monazite of the Mont Mort metapelite, located in the Ruitor zone of the Bernard nappe complex, and was interpreted as the timing of amphibolite facies metamorphism (Bussy et al. 1996b; Giorgis et al. 1999). Hence a Variscan amphibolite facies metamorphism was followed by strong greenschist facies retrogression, largely erasing the amphibolite facies parageneses. This Variscan evolution is quite similar to what has been observed in the Helvetic basement units (e.g., Bussy et al. 2000; Schaltegger et al. 2003; von Raumer et al. 2009).

The two metasedimentary samples 618 and 644 and the Ordovician orthogneiss sample 636 contain zircons with up to 20 µm thick, CL-bright outermost rims (Fig. 3). Given the youngest detrital zircon grains in samples 618 and 644 and the intrusion age of sample 636, these bright rims have to be younger than ~480 Ma. Since the LA-ICP-MS technique is at its limit with respect to the spot size, only one analysis of such a rim gave a meaningful result of ($^{206}Pb/^{238}U$) 355 ± 19 Ma (E14, sample 644, Fig. 3e). A contribution of old inherited zircon material to the laser spot analysis cannot be totally excluded, which makes this age a maximum age. Consequently, these zircon rims most probably reflect the fluid-driven metamorphic overprint during the Variscan cycle. Obviously, the Thyon orthogneiss (sample 667) was not affected by new zircon growth, which may be explained by the lack of fluids during metamorphism, or it simply escaped Variscan metamorphism.

The late- to post-Variscan evolution can be deduced from the Permian orthogneiss sample 687 and from the three zircons of sample 618 lacking an outermost highly luminescent rim (E4, E16 and E29 in Fig. 3d). Zircons E4 and E29 seem to be of key significance: The analysis on the central part of the highly luminescent, irregularly-textured zircon E4 yielded an age of 281 ± 5 Ma. Zircon E29 contains a highly luminescent core (300 ± 7 Ma), continuously grading into an oscillatory zoned moderately luminescent rim (253 ± 5 Ma), which is generally typical of igneous zircon grown from a melt or a hydrothermal fluid (Corfu et al. 2003). Since a Permian or younger age of sedimentation can be excluded for the SOPA (see also, e.g., Thélin et al. 1993; Sartori et al. 2006), these zircons cannot be of detrital origin, but must have developed in the course of a Permian magmatometamorphic cycle. Combining the observations on zircons E4 and E29 with the analysis of an irregular bright rim truncating an inner core on zircon E16 (293 ± 7 Ma, 85 % concordance), together with the weighted mean $^{206}Pb/^{238}U$ ages calculated for zircon populations within sample 687 (290 ± 4 and 272 ± 4 Ma), indicates a clear signature of post-Variscan thermal activity that it is well known from all over Europe (e.g., Wilson et al. 2004; Timmerman 2008, and references therein). Numerous Carboniferous-Permian intrusions are reported from different basement units within the Alps (e.g., Bonin et al. 1993). They are generally interpreted to be the result of several extensional stages due to readjustment of the thickened continental lithosphere at late stages of and subsequently to the Variscan orogeny. The large spread of post-Variscan Permian ages within our dataset (300–272 Ma) points to a long-lasting magmatometamorphic cycle in the Permian, as it is similarly observed in the Briançon-derived Suretta nappe of eastern Switzerland (Scheiber et al. 2013) and in the External Crystalline Massifs of the Helvetic domain (e.g., Schaltegger 1997). Granitoid intrusions such as the Randa orthogneiss and the orthogneiss from Le Bautsé (sample 687) must have brought enough fluids and heat to produce locally overgrowths on zircons and probably precipitation of new zircon crystals within the surrounding metasediments. Surprisingly, the white mica ages were only locally reset by this

heating, mostly in the proximity of the Randa orthogneiss (Fig. 1b). For the area of sample 618, where new Permian zircon growth was observed, no age constraints on the mica populations are available, but it is likely that the age was reset in this particular sample.

The youngest $^{206}Pb/^{238}U$ dates (younger than 272 ± 4 Ma, which is the weighted mean of the youngest grains interpreted as magmatic, Fig. 4b) may reflect disturbance and partial Pb-loss of the U–Pb system due to post-crystallization thermal events during late Permian to early Triassic times (e.g., Schaltegger and Gebauer 1999; Marotta and Spalla 2007) or during Alpine deformation. In the Siviez-Mischabel nappe, the Alpine main deformation took place between 41 and 36 Ma (Markley et al. 1998, 2002) and did not exceed (high pressure) greenschist facies conditions (Bousquet et al. 2004; Oberhänsli et al. 2004). Alpine deformation in the basement unit is relatively weak and represented by localized shear zones and open folds reorienting the Variscan main foliation. Zircon spot analyses (<90 % concordant) from the imbricated orthogneiss slices (samples 636 and 687) and from overthrust metasediments (sample 644) indicate a young disturbance of the U–Pb system, most probably reflecting the weak Alpine overprint.

7 Conclusions

The basement of the Siviez-Mischabel nappe records not only all Paleozoic magmatic events known in the basement of the Alps, but also the most prominent pre-Cambrian cycles of crustal growth observed within the European Variscides.

Prevailing Pan-African (Cadomian) ages among a range of Archean to Proterozoic ages suggest that the albitic metasediments within the Siviez-Mischabel nappe were deposited in late Cambrian time and consist of material predominantly derived from a Pan-African source, which involved Archean to Proterozoic crustal components. The Thyon orthogneiss and one orthogneiss slice (Illsee) represent Cambro-Ordovician intrusions into the pre-Cambrian basement and possibly into the Cambrian metasediments and are probably related to extensional tectonics during break-up of Gondwana. Subsequently, high-pressure metamorphism formed the Siviez-Mischabel (retro-) eclogites either during this orogenic cycle (480–440) or later during early stages of the Variscan cycle. The entire Siviez-Mischabel basement was strongly affected by Carboniferous amphibolite facies metamorphism, followed by greenschist facies retrogression and Carboniferous-Permian thermal heating related to the Variscan cycle. The latter triggered a range of intrusions (e.g., Randa orthogneiss and orthogneiss Le Bautsé) and recrystallization processes in zircons of the surrounding metasediments. Zircons from the Thyon orthogneiss, however, remained unaffected by the entire post-Cambrian evolution.

Acknowledgments This study was funded by the Swiss National Science Foundation (Grant No. 200020–122143). We thank Urs Klötzli and François Bussy for constructive reviews and comments.

References

Abouchami, W., Boher, M., Michard, A., & Albarede, F. (1990). A major 2.1 Ga event of mafic magmatism in West Africa: An early stage of crustal accretion. *Journal of Geophysical Research, 95*, 17605–17629.

Andersen, T. (2005). Detrital zircons as tracers of sedimentary provenance: Limiting conditions from statistics and numerical simulation. *Chemical Geology, 216*, 249–270.

Ballèvre, M., Fourcade, S., Capdevila, R., Peucat, J. J., Cocherie, A., & Fanning, C. M. (2012). Geochronology and geochemistry of Ordovician felsic volcanism in the Southern Armorican Massif (Variscan belt, France): Implications for the breakup of Gondwana. *Gondwana Research, 21*, 1019–1036.

Bearth, P. (1963). Contribution à la subdivision tectonique et stratigraphique du Cristallin de la nappe du Grand-St-Bernard dans le Valais (Suisse). In: M. Durand Delga (Ed.), *Livre à la Mémoire du Professeur Paul Fallot* (pp. 407–418). Mémoire hors-série, Société géologique de France, t. II, (1960–1963).

Bearth, P. (1978). Blatt 71 St.Niklaus, 1:25'000. *Geologischer Atlas der Schweiz, Karte 1308*, swisstopo, Wabern.

Bertrand, J. M., Guillot, F., & Leterrier, J. (2000a). Âge Paléozoique inférieur (U-Pb sur zircon) de métagranophyres de la nappe du Grand-Saint-Bernard (zona interna, vallée d'Aoste, Italie). *Comptes Rendus de l'Académie des sciences-Series IIA-Earth and Planetary Science, 330*, 473–478.

Bertrand, J. M., Pidgeon, R. T., & Leterrier, J. (2000b). SHRIMP and IDTIMS U-Pb zircon ages of the pre-Alpine basement in the Internal Western Alps (Savoy and Piemont). *Schweizerische Mineralogische und Petrographische Mitteilungen, 80*, 225–248.

Biino, G. (1995). Pre-Variscan evolution of the eclogitised mafic rocks from the Helvetic basement of the central Alps. *European Journal of Mineralogy, 7*, 57–70.

Bleiner, D., & Günther, D. (2001). Theoretical description and experimental observation of aerosol transport processes in laser ablation inductively coupled plasma mass spectrometry. *Journal of Analytical Atomic Spectrometry, 16*, 449–456.

Boher, M., Abouchami, W., Michard, A., Albarede, F., & Arndt, N. T. (1992). Crustal Growth in West Africa at 2.1 Ga. *Journal of Geophysical Research, 97*, 345–369.

Bonin, B., Brändlein, P., Bussy, F., Desmons, J., Eggenberger, U., Finger, F., et al. (1993). Late Variscan magmatic evolution of the Alpine basement. In J. F. von Raumer & F. Neubauer (Eds.), *Pre-Mesozoic Geology in the Alps* (pp. 171–201). Berlin: Springer.

Bousquet, R., Engi, M., Gosso, G., Oberhänsli, R., Berger, A., Spalla, M. I., et al. (2004). Explanatory notes to the map: Metamorphic structure of the Alps. Transition from the western to the central Alps. *Mitteilungen der Österreichischen Mineralogischen Gesellschaft, 149*, 145–156.

Bowring, S. A., Schoene, B., Crowley, J. L., Ramezani, J., & Condon D. J. (2006). High-precision U-Pb zircon geochronology and the stratigraphic record: Progress and promise. In: T. D. Olszewski

(Ed.), *Geochronology: Emerging opportunities* (pp. 25–46). Paleontological Society Short Course.

Burri, M. (1983). Le front du Grand St-Bernard du val d'Hérens au val d'Aoste. *Eclogae Geologicae Helvetiae, 76*, 469–490.

Burri, M., Fricker, P., Grasmück, K., Marro, C., & Oulianoff, N. (1992). Blatt 91 Orsières, 1:25'000. *Geologischer Atlas der Schweiz, Karte 1345,* swisstopo, Wabern.

Bussien, D., Bussy, F., Magna, T., & Masson, H. (2011). Timing of Palaeozoic magmatism in the Maggia and Sambuco nappes and paleogeographic implications (Central Lepontine Alps). *Swiss Journal of Geosciences, 104*, 1–29.

Bussy, F., & Cadoppi, P. (1996). U-Pb zircon dating of granitoids from the Dora-Maira massif (western Italian Alps). *Schweizerische Mineralogische und Petrographische Mitteilungen, 76*, 217–233.

Bussy, F., Derron, M. H., Jacquod, J., Sartori, M., & Thélin, P. (1996a). The 500 Ma-old Thyon metagranite: A new A-type granite occurrence in the western Penninic Alps (Wallis, Switzerland). *European Journal of Mineralogy, 8*, 565–575.

Bussy, F., Hernandez, J., & von Raumer, J. F. (2000). Bimodal magmatism as a consequence of the post-collisional readjustment of the thickened Variscan continental lithosphere (Aiguilles Rouges - Mont Blanc Massifs, Western Alps). *Geological Society of America Special Papers, 350*, 221–233.

Bussy, F., Sartori, M., & Thélin, P. (1996b). U-Pb zircon dating in the middle Penninic basement of the Western Alps (Valais, Switzerland). *Schweizerische Mineralogische und Petrographische Mitteilungen, 76*, 81–84.

Cavargna-Sani, M., Epard, J.-L., Bussy, F., & Ulianov, A. (2013). Basement lithostratigraphy of the Adula nappe: implications for Palaeozoic evolution and Alpine kinematics. *International Journal of Earth Sciences*. doi:10.1007/s00531-013-0941-1 (in press).

Cawood, P. A., Hawkesworth, C. J., & Dhuime, B. (2012). Detrital zircon record and tectonic setting. *Geology, 40*, 875–878.

Corfu, F., Hanchar, J. M., Hoskin, P. W. O., & Kinny, P. (2003). Atlas of zircon textures. In: J. M. Hanchar & P. W. O. Hoskin (Eds.), *Reviews in Mineralogy and Geochemistry* (vol. 53: Zircon, pp. 469–500). Washington: Mineral Society of America.

Dickinson, W. R., & Gehrels, G. E. (2009). Use of U–Pb ages of detrital zircons to infer maximum depositional ages of strata: A test against a Colorado Plateau Mesozoic database. *Earth and Planetary Science Letters, 288*, 115–125.

Díez Fernández, R., Castiñeiras, P., & Gómez Barreiro, J. (2012). Age constraints on Lower Paleozoic convection system: Magmatic events in the NW Iberian Gondwana margin. *Gondwana Research, 21*, 1066–1079.

Eisele, J., Geiger, S., & Rahn, M. (1997). Chemical characterization of metabasites from the Turtmann valley (Valais, Switzerland): implications for their protoliths and geotectonic origin. *Schweizerische Mineralogische und Petrographische Mitteilungen, 77*, 403–417.

Ellenberger, F. (1952). Sur l'extension des faciès Briançonnais en Suisse, dans les Préalpes médianes et les Pennides. *Eclogae Geologicae Helvetiae, 45*, 285–286.

Ellenberger, F. (1953). La Série du Barrhorn et les rétrocharriages penniques. *Comptes Rendus de l'Académie des sciences, 236*, 218–220.

Escher, A. (1988). Structure de la nappe du Grand Saint-Bernard entre le val de Bagnes et les Mischabel. *Rapport géologique du Service hydrologique et géologique national, 7*.

Fernández-Suárez, J., Gutiérrez Alonso, G., & Jeffries, T. E. (2002). The importance of along-margin terrane transport in northern Gondwana: insights from detrital zircon parentage in Neoproterozoic rocks from Iberia and Brittany. *Earth and Planetary Science Letters, 204*, 75–88.

Finger, F., Roberts, M. P., Haunschmid, B., Schermaier, A., & Steyrer, H. P. (1997). Variscan granitoids of central Europe: Their typology, potential sources and tectonothermal relations. *Mineralogy and Petrology, 61*, 67–96.

Franke, W. (2006). The Variscan orogen in Central Europe: Construction and collapse. *Geological Society, London, Memoirs, 32*, 333–343.

Gabus, J. H., Weidmann, M., Bugnon, P.-C., Burri, M., Sartori, M., & Marthaler, M. (2008a). Feuille 111 Sierre, 1:25'000. *Atlas géol. Suisse, Carte 1287*, swisstopo, Wabern.

Gabus, J. H., Weidmann, M., Burri, M., & Sartori, M. (2008b). Notice explicative - Feuille 111 Sierre. *Atlas géologique de la Suisse 1:25'000, Carte 1287*, swisstopo, Wabern.

Galli, A., Le Bayon, B., Schmidt, M., Burg, J. P., Reusser, E., Sergeev, S., et al. (2012). U-Pb zircon dating of the Gruf Complex: Disclosing the late Variscan granulitic lower crust of Europe stranded in the Central Alps. *Contributions to Mineralogy and Petrology, 163*, 353–378.

Gauthiez, L., Bussy, F., Ulianov, A., Gouffon, Y., & Sartori, M. (2011). *Ordovician mafic magmatism in the Métailler Formation of the Mont-Fort nappe (Middle Penninic domain, western Alps)—Geodynamic implications* (pp. 110–111). 9th Swiss geoscience meeting, Zürich, Switzerland.

Gebauer, D. (1993). The pre-Alpine evolution of the continental crust of the Central Alps—An overview. In J. Von Raumer & F. Neubauer (Eds.), *Pre-Mesozoic Geology in the Alps* (pp. 93–117). Berlin: Springer.

Gebauer, D., Williams, I. S., Compston, W., & Grünenfelder, M. (1989). The development of the Central European continental crust since the Early Archaean based on conventional and ion-microprobe dating of up to 3.84 b.y. old detrital zircons. *Tectonophysics, 157*, 81–96.

Genier, F., Epard, J.-L., Bussy, F., & Magna, T. (2008). Lithostratigraphy and U–Pb zircon dating in the overturned limb of the Siviez-Mischabel nappe: A new key for Middle Penninic nappe geometry. *Swiss Journal of Geosciences, 101*, 431–452.

Giacomini, F., Braga, R., Tiepolo, M., & Tribuzio, R. (2007). New constraints on the origin and age of Variscan eclogitic rocks (Ligurian Alps, Italy). *Contributions to Mineralogy and Petrology, 153*, 29–53.

Giorgis, D., Thélin, P., Stampfli, G. M., & Bussy, F. (1999). The Mont-Mort metapelites: Variscan metmorphism and geodynamic context (Briançonnais basement, Western Alps, Switzerland). *Schweizerische Mineralogische und Petrographische Mitteilungen, 79*, 381–389.

Guillot, F., Schaltegger, U., Bertrand, J., Deloule, É., & Baudin, T. (2002). Zircon U–Pb geochronology of Ordovician magmatism in the polycyclic Ruitor Massif (Internal W Alps). *International Journal of Earth Sciences, 91*, 964–978.

Jackson, S. E., Pearson, N. J., Griffin, W. L., & Belousova, E. A. (2004). The application of laser ablation-inductively coupled plasma-mass spectrometry to in situ U–Pb zircon geochronology. *Chemical Geology, 211*, 47–69.

Jackson, N. J., & Ramsay, C. R. (1980). What is the "Pan-African"? A consensus is needed. *Geology, 8*, 210–211.

Kooijman, E., Berndt, J., & Mezger, K. (2012). U–Pb dating of zircon by laser ablation ICP-MS: Recent improvements and new insights. *European Journal of Mineralogy, 24*, 5–21.

Krawczyk, C. M., McCann, T., Cocks, L. R. M., England, R. W., McBride, J. H., & Wybraniec, S. (2008). Caledonian tectonics. In T. McCann (Ed.), *The geology of Central Europe* (Vol. 1: Precambrian and Paleozoic, pp. 303–381). London: Geological Society.

Kroner, U., Mansy, J.-L., Mazur, S., Aleksandrowski, P., Hann, H. P., Huckriede, H., et al. (2008). Variscan tectonics. In T. McCann

(Ed.), *The geology of Central Europe* (Vol. 1: Precambrian and Paleozoic, pp. 599–664). London: Geological Society.

Ludwig, K. R. (2008). User's manual for Isoplot 3.70. A geochronological toolkit for microsoft excel. *Berkeley Geochronology Center, Special Publication, 4*.

Markley, M. J., Teyssier, C., & Caby, R. (1999). Re-examining Argand's view of the Siviez-Mischabel nappe. *Journal of Structural Geology, 21*, 1119–1124.

Markley, M. J., Teyssier, C., & Cosca, M. (2002). The relation between grain size and $^{40}Ar/^{39}Ar$ date for Alpine white mica from the Siviez-Mischabel Nappe, Switzerland. *Journal of Structural Geology, 24*, 1937–1955.

Markley, M. J., Teyssier, C., Cosca, M. A., Caby, R., Hunziker, J. C., & Sartori, M. (1998). Alpine deformation and $^{40}Ar/^{39}Ar$ geochronology of synkinematic white mica in the Siviez-Mischabel Nappe, western Pennine Alps, Switzerland. *Tectonics, 17*, 407–425.

Marotta, A. M., & Spalla, M. I. (2007). Permian-Triassic high thermal regime in the Alps: Result of late Variscan collapse or continental rifting? Validation by numerical modeling. *Tectonics, 26*, TC4016.

Marthaler, M., Sartori, M., & Escher, A. (2008). Feuille 122 Vissoie, 1:25'000. *Atlas géol. Suisse, Carte 1307*, swisstopo, Wabern.

Meinhold, G., Morton, A. C., & Avigad, D. (2013). New insights into peri-Gondwana paleogeography and the Gondwana super-fan system from detrital zircon U–Pb ages. *Gondwana Research, 23*, 661–665.

Monié, P. (1990). Preservation of Hercynian $^{40}Ar/^{39}Ar$ ages through high-pressure low-temperature Alpine metamorphism in the Western Alps. *European Journal of Mineralogy, 2*, 343–361.

Neubauer, F. (2002). Evolution of late Neoproterozoic to early Paleozoic tectonic elements in Central and Southeast European Alpine mountain belts: review and synthesis. *Tectonophysics, 352*, 87–103.

Oberhänsli, R., Bousquet, R., Engi, M., Goffé, B., Gosso, G., Handy, M. R., Höck, V., Koller, F., Lardeaux, J.-M., Polino, R., Rossi, P., Schuster, R., Schwartz, S., & Spalla, M. I. (2004). Metamorphic structure of the Alps, 1:1,000,000. sGMW: Commission for the Geological Map of the World.

Oberli, F., Meier, M., & Biino, G. (1994). Time constraints on the pre-Variscan magmatic/metamorphic evolution of the Gotthard and Tavetsch units derived from single-zircon U–Pb results. *Schweizerische Mineralogische und Petrographische Mitteilungen, 74*, 483–488.

Pfeifer, H. R., Biino, G., Ménot, R. P., & Stille, P. (1993). Ultramafic rocks in the pre-Mesozoic basement of the Central and external Western Alps. In J. F. von Raumer & F. Neubauer (Eds.), *Pre-Mesozoic Geology in the Alps* (pp. 119–143). Berlin: Springer.

Pin, C., Kryza, R., Oberc-Dziedzic, T., Mazur, S., Turniak, K., & Waldhausrová, J. (2007). The diversity and geodynamic significance of Late Cambrian (ca. 500 Ma) felsic anorogenic magmatism in the northern part of the Bohemian Massif: A review based on Sm-Nd isotope and geochemical data. *Geological Society of America Special Papers, 423*, 209–229.

Rahn, M. (1991). Eclogites from the Minugrat, Siviez-Mischabel nappe (Valais, Switzerland). *Schweizerische Mineralogische und Petrographische Mitteilungen, 71*, 415–426.

Rino, S., Kon, Y., Sato, W., Maruyama, S., Santosh, M., & Zhao, D. (2008). The Grenvillian and Pan-African orogens: World's largest orogenies through geologic time, and their implications on the origin of superplume. *Gondwana Research, 14*, 51–72.

Rubatto, D., Ferrando, S., Compagnoni, R., & Lombardo, B. (2010). Carboniferous high-pressure metamorphism of Ordovician protoliths in the Argentera Massif (Italy), Southern European Variscan belt. *Lithos, 116*, 65–76.

Rubatto, D., Schaltegger, U., & Lombardo, B. (2001). Complex Paleozoic magmatic and metamorphic evolution in the Argentera Massif (Western Alps) resolved with U–Pb dating. *Schweizerische Mineralogische und Petrographische Mitteilungen, 81*, 213–228.

Sartori, M. (1987a). Blocs basculés briançonnais en relation avec leur socle originel dans la nappe de Siviez-Mischabel (Valais, Suisse). *Comptes Rendus de l'Académie des Sciences, 305*, 999–1005.

Sartori, M. (1987b). Structure de la zone du Combin entre les Diablons et Zermatt (Valais). *Eclogae Geologicae Helvetiae, 80*, 789–814.

Sartori, M. (1990). L'unité du Barrhorn (Zone pennique, Valais, Suisse). *Mémoires de Géologie, Lausanne, 6*.

Sartori, M., Burri, M., Epard, J. L., Masson, H., & Pasquier, J. B. (2011). Feuille 130 Sion, 1:25'000. *Atlas géol. Suisse, Carte 1306*, swisstopo, Wabern.

Sartori, M., & Epard, J. L. (2011). Notice explicative - Feuille 130 Sion. *Atlas géologique de la Suisse 1:25'000, Carte 1306*, swisstopo, Wabern.

Sartori, M., Gouffon, Y., & Marthaler, M. (2006). Harmonisation et définition des unités lithostratigraphiques briançonnaises dans les nappes penniques du Valais. *Eclogae Geologicae Helvetiae, 99*, 363–407.

Sartori, M., & Thélin, P. (1987). Les schistes oeillés albitiques de Barneuza (Nappe de Siviez-Mischabel, Valais, Suisse). *Schweizerische Mineralogische und Petrographische Mitteilungen, 67*, 229–256.

Schaer, J.-P. (1959). Géologie de la partie septentrionale de l'éventail de Bagnes. *Archives des Sciences, Genève, 12*, 473–620.

Schaltegger, U. (1997). Magma pulses in the Central Variscan Belt: Episodic melt generation and emplacement during lithospheric thinning. *Terra Nova, 9*, 242–245.

Schaltegger, U., Albrecht, J., & Corfu, F. (2003). The Ordovician orogeny in the Alpine basement: constraints from geochronology and geochemistry in the Aar Massif (Central Alps). *Schweizerische Mineralogische und Petrographische Mitteilungen, 83*, 183–195.

Schaltegger, U., & Gebauer, D. (1999). Pre-Alpine geochronology of the Central, Western and Southern Alps. *Schweizerische Mineralogische und Petrographische Mitteilungen, 79*, 79–87.

Scheiber, T., Berndt, J., Heredia, B. D., Mezger, K., & Pfiffner, O. A. (2013a). Episodic and long-lasting Paleozoic felsic magmatism in the pre-Alpine basement of the Suretta nappe (eastern Swiss Alps). *International Journal of Earth Sciences, 102*, 2097–2115.

Scheiber, T., Pfiffner, A., & Schreurs, G. (2013b). Upper crustal deformation in continent–continent collision: a case study from the Bernard nappe complex (Valais, Switzerland). *Tectonics 32*, 1320–1342.

Schulz, B. (2008). Basement of the Alps. In T. McCann (Ed.), *The geology of Central Europe* (Vol. 1: Precambrian and Paleozoic, pp. 79–83). London: Geological Society.

Soom, M. (1990). Abkühlungs- und Hebungsgeschichte der Externmassive und der penninischen Decken beidseits der Simplon-Rhone-Linie seit dem Oligozän: Spaltspurdatierungen an Apatit/Zirkon und K-Ar-Datierungen an Biotit/Muskowit (Westliche Zentralalpen). *Ph.D. dissertation*, Univ. Bern, Switzerland.

Stacey, J. S., & Kramers, J. D. (1975). Approximation of terrestrial lead isotope evolution by a two-stage model. *Earth and Planetary Science Letters, 26*, 207–221.

Stampfli, G. M., Mosar, J., Marquer, D., Marchant, R., Baudin, T., & Borel, G. (1998). Subduction and obduction processes in the Swiss Alps. *Tectonophysics, 296*, 159–204.

Steck, A., Bigioggero, B., dal Piaz, G. V., Escher, A., Martinotti, G., & Masson, H. (1999). Carte tectonique des Alpes de Suisse

occidentale, 1:100,000. *Carte géologique spéciale N°123* (*4 feuilles*), swisstopo, Wabern.

Steiger, R. H., & Jäger, E. (1977). Subcommission on geochronology: Convention on the use of decay constants in geo- and cosmochronology. *Earth and Planetary Science Letters, 36*, 359–362.

Taylor, S. R., & McLennan, S. M. (1985). *The continental crust: its composition and evolution*. Oxford: Blackwell. 311 pp.

Thélin, P. (1987). Nature originelle des gneiss oeillés de Randa (Nappe de Siviez-Mischabel, Valais). *Mémoires de la Société Vaudoise des Sciences Naturelles, 104* (Vol. 18).

Thélin, P. (1989). Essai de chronologie magmatico-métamorphique dans le socle de la nappe du Grand Saint-Bernard: quelques points de repère. *Schweizerische Mineralogische und Petrographische Mitteilungen, 69*, 193–204.

Thélin, P., Sartori, M., Burri, M., Gouffon, Y., & Chessex, R. (1993). The pre-Alpine basement of the Briançonnais (Wallis, Switzerland). In J. F. von Raumer & F. Neubauer (Eds.), *Pre-Mesozoic Geology in the Alps* (pp. 297–315). Berlin: Springer.

Thélin, P., Sartori, M., Lengeler, R., & Schaerer, J.-P. (1990). Eclogites of Paleozoic or early Alpine age in the basement of the Penninic Siviez-Mischabel nappe, Wallis, Switzerland. *Lithos, 25*, 71–88.

Thöni, M. (2006). Dating eclogite-facies metamorphism in the Eastern Alps—Approaches, results, interpretations: A review. *Mineralogy and Petrology, 88*, 123–148.

Timmerman, M. J. (2008). Palaeozoic magmatism. In T. McCann (Ed.), *The geology of Central Europe* (Vol. 1: Precambrian and Paleozoic, pp. 665–748). London: Geological Society.

Vallet, J.-M. (1950). Etude géologique et pétrographique de la partie inférieure du Val d'Hérens et du Val d'Hérémence (Valais). *Schweizerische Mineralogische und Petrographische Mitteilungen, 30*, 322–476.

Vermeesch, P. (2004). How many grains are needed for a provenance study? *Earth and Planetary Science Letters, 224*, 441–451.

Vermeesch, P. (2012). On the visualisation of detrital age distributions. *Chemical Geology, 312–313*, 190–194.

von Quadt, A. (1992). U–Pb zircon and Sm–Nd geochronology of mafic and ultramafic rocks from the central part of the Tauern Window (eastern Alps). *Contributions to Mineralogy and Petrology, 110*, 57–67.

von Raumer, J. F., Bussy, F., Schaltegger, U., Schulz, B., & Stampfli, G. M. (2013). Pre-Mesozoic Alpine basements—Their place in the European Paleozoic framework. *Geological Society of America Bulletin, 125*, 89–108.

von Raumer, J., Bussy, F., & Stampfli, G. M. (2009). The Variscan evolution in the External massifs of the Alps and place in their Variscan framework. *Comptes Rendus Geoscience, 341*, 239–252.

von Raumer, J., Stampfli, G. M., Borel, G., & Bussy, F. (2002). Organization of pre-Variscan basement areas at the north-Gondwanan margin. *International Journal of Earth Sciences, 91*, 35–52.

von Raumer, J. F., Stampfli, G. M., & Bussy, F. (2003). Gondwana-derived microcontinents—The constituents of the Variscan and Alpine collisional orogens. *Tectonophysics, 365*, 7–22.

Wiedenbeck, M., Allé, P., Corfu, F., Griffin, W. L., Meier, M., Oberli, F., et al. (1995). Three natural zircon standards for U–Th–Pb, Lu–Hf, trace element and REE analyses. *Geostandards Newsletter, 19*, 1–23.

Wiedenbeck, M., Hanchar, J. M., Peck, W. H., Sylvester, P., Valley, J., Whitehouse, M., et al. (2004). Further characterisation of the 91500 zircon crystal. *Geostandards and Geoanalytical Research, 28*, 9–39.

Wilson, M., Neumann, E.-R., Davies, G. R., Timmerman, M. J., Heeremans, M., & Larsen, B. T. (2004). Permo-Carboniferous magmatism and rifting in Europe: Introduction. *Geological Society, London, Special Publications, 223*, 1–10.

Zingg, M. (1989). Die Siviez-Mischabel Decke - Entstehung und Entwicklung eines Altkristallins und seiner Vererzungen (Wallis, Schweiz). *Ph.D. dissertation*, Zürich.